⌘ *Author's Choice*

THE JOURNAL OF BIOLOGICAL CHEMISTRY VOL. 287, NO. 14, pp. 11164–11173, March 30, 2012

Remodeling of Lipid Droplets during Lipolysis and Growth in Adipocytes*[S]

Received for publication, October 24, 2011, and in revised form, January 31, 2012 Published, JBC Papers in Press, February 6, 2012, DOI 10.1074/jbc.M111.316794

Margret Paar[‡1], Christian Jüngst[§1,2], Noemi A. Steiner[‡], Christoph Magnes[¶], Frank Sinner[¶], Dagmar Kolb[‖], Achim Lass[‡], Robert Zimmermann[‡], Andreas Zumbusch[§], Sepp D. Kohlwein[‡], and Heimo Wolinski[‡3]

From the [‡]Institute of Molecular Biosciences, Lipidomics Research Center LRC Graz, University of Graz, 8010 Graz, Austria, the [§]Department of Chemistry, University of Konstanz, 78457 Konstanz, Germany, [¶]HEALTH, Institute for Biomedicine and Health Sciences, Joanneum Research, 8036 Graz, Austria, and the [‖]Institute of Cell Biology, Histology and Embryology, and ZMF, Center for Medical Research, Medical University of Graz, 8010 Graz, Austria

Background: Micro-lipid droplets (mLDs) appear in adipocytes upon lipolytic stimulation. LDs may grow by spontaneous, homotypic fusion.
Results: Scavenging of fatty acids prevents mLD formation. LDs grow by a slow transfer of lipids between LDs.
Conclusion: mLDs form due to fatty acid overflow. LD growth is a controlled process.
Significance: Novel mechanistic insights into LD remodeling are provided.

Synthesis, storage, and turnover of triacylglycerols (TAGs) in adipocytes are critical cellular processes to maintain lipid and energy homeostasis in mammals. TAGs are stored in metabolically highly dynamic lipid droplets (LDs), which are believed to undergo fragmentation and fusion under lipolytic and lipogenic conditions, respectively. Time lapse fluorescence microscopy showed that stimulation of lipolysis in 3T3-L1 adipocytes causes progressive shrinkage and almost complete degradation of all cellular LDs but without any detectable fragmentation into micro-LDs (mLDs). However, mLDs were rapidly formed after induction of lipolysis in the absence of BSA in the culture medium that acts as a fatty acid scavenger. Moreover, mLD formation was blocked by the acyl-CoA synthetase inhibitor triacsin C, implicating that mLDs are synthesized *de novo* in response to cellular fatty acid overload. Using label-free coherent anti-Stokes Raman scattering microscopy, we demonstrate that LDs grow by transfer of lipids from one organelle to another. Notably, this lipid transfer between closely associated LDs is not a rapid and spontaneous process but rather occurs over several h and does not appear to require physical interaction over large LD surface areas. These data indicate that LD growth is a highly regulated process leading to the heterogeneous LD size distribution within and between individual cells. Our findings suggest that lipolysis and lipogenesis occur in parallel in a cell to prevent cellular fatty acid overflow. Furthermore, we propose that formation of large LDs requires a yet uncharacterized protein machinery mediating LD interaction and lipid transfer.

Most eukaryotic organisms deal with a typically fluctuating food supply by storing or mobilizing lipids as an energy source. Malfunction of the synthesis or degradation of fat stores is linked to prevalent diseases, such as obesity, type II diabetes, or various forms of lipodystrophy (1). In mammals, adipose tissue functions as the major energy depot of the body. Excess fatty acids (FAs)[4] and sterols are stored as neutral lipids (mostly as triacylglycerol (TAG) as well as steryl esters) in cytosolic lipid droplets (LDs), which are mobilized by regulated lipolytic breakdown in response to specific nutritional needs of the cell or organism. The LD surface consists of a phospholipid monolayer harboring a set of enzymes and regulatory proteins that catalyze the highly metabolically controlled synthesis and mobilization of fat stores. Compartmentation of nonpolar neutral lipids into LDs ensures their physiological accessibility and, thus, plays a central and critical role in lipid homeostasis. Neutral lipid turnover is accompanied by a significant remodeling of LDs, and both the appearance of microlipid droplets (mLDs) during breakdown of neutral lipids and growth of the organelles by fusion events have been discussed as fundamental processes required for efficient mobilization and storage of fat in adipocytes (2–6).

A number of studies have reported that in differentiated murine (3T3-L1) adipocytes, large perinuclear LDs fragment and disperse into smaller mLDs in response to lipolytic stimulation (7–10). Such a fragmentation process is expected to drastically increase the surface/volume ratio of the LDs, leading to more efficient degradation of stored neutral lipids by LD-associated lipases. Dispersion of LDs was also found to affect the localization of perilipin, one of the main regulators of LD turn-

* This work was supported in part by grants from the Austrian Science Funds, FWF, Project LIPOTOX F3005-B12 (to S. D. K.) and Ph.D. Program Molecular Enzymology, Project W901-B05, and the Austrian Federal Government for Science and Research (Project GOLD, in the framework of the Austrian Genome Program GEN-AU) (to S. D. K. and H. W.).
⌘ *Author's Choice*—Final version full access.
[S] This article contains supplemental Movies S1–S4.
[1] Both authors contributed equally to this work.
[2] Supported by contract research "Methoden für die Lebenswissenschaften" of the Baden-Württemberg Stiftung and a personal scholarship from the Konstanz Research School Chemical Biology.
[3] To whom correspondence should be addressed: Institute of Molecular Biosciences, Lipidomics Research Center LRC Graz, University of Graz, Humboldtstrasse 50/II, 8010 Graz, Austria. Tel.: 43-316-380-5489; Fax: 43-316-380-9854; E-mail: heimo.wolinski@uni-graz.at.

[4] The abbreviations used are: FA, fatty acid; TAG, triacylglycerol; LD, lipid droplet; mLD, micro-LD; nLD, nano-LD; CARS, coherent anti-Stokes Raman scattering; ER, endoplasmic reticulum; ATGL, adipose triglyceride lipase; NA, numerical aperture.

over, as well as of hormone-sensitive lipase. Both proteins are restricted to a subpopulation of dispersed LDs, and it was suggested that mLDs that emerge under lipolytic conditions may represent an active pool of LDs from which neutral lipids are mobilized (10). Controversially, however, a recent time lapse study using label-free coherent anti-Stokes Raman scattering (CARS) microscopy showed that in differentiated 3T3-L1 adipocytes, mLDs appeared scattered throughout the cytosol upon lipolytic stimulation but were not detected at specific regions neighboring large LDs as would be expected if they originated by LD fragmentation. It was suggested that these LDs may instead derive from other organelles, such as the endoplasmic reticulum (ER), rather than from existing LDs. On the other hand, "nano-LDs" (nLDs), which may not be detectable by CARS microscopy, may split off from larger LDs and subsequently fuse to give rise to mLDs that are found dispersed in the cytosol (11).

Furthermore, controversy also exists concerning the mode of LD growth. Homotypic interaction between LDs of 3T3-L1 adipocytes may indeed cause fusion of the organelles; this process does not require TAG synthesis but depends on microtubules and the motor protein dynein (12, 13). Furthermore, it was suggested that SNARE proteins mediate LD fusion (14). However, in another study, fusion of LDs could not be observed in the same cell type under conditions of induced lipid synthesis. According to this study, nascent LDs may form at the cellular periphery and move toward larger perinuclear "storage" LDs. Such LDs enlarge during their movement without observable fusion events, presumably by synthesis of new TAG directly on the LD (15). Both diacylglycerol and diacylglycerol acyltransferase 2 catalyzing the conversion of diacylglycerol to TAG were detected in the vicinity of lipid droplets both in 3T3-L1 and COS7 cells, suggesting that LDs may also grow by biosynthesis of TAG near LDs and direct incorporation into existing LDs (16). Moreover, it was shown that LDs of rat hepatoma cells grow by incorporation of esterified cholesterol into existing lipid droplets rather than by fusion events (17). A recent analysis of LD fusion in murine adipocytes using time lapse light microscopy showed that fast organelle fusion can be stimulated by various drugs, which, however, appears to be a rare event in untreated cells (18). Finally, in addition to *de novo* synthesis and fusion, LDs may also grow by a dynamic interaction and gradual (regulated) transfer of TAG between nascent and preformed LDs, as shown in primary mouse hepatocytes. In these cells, transient fusion and fission events may occur upon contact of two closely associated LDs (19).

In this study, we applied high resolution long term four-dimensional live cell imaging of murine adipocytes and human adipose-derived stem cells to monitor the breakdown as well as the formation of LDs. Our results demonstrate that efficient degradation of LDs is not accompanied by fragmentation and dispersion of LDs in 3T3-L1 adipocytes but rather leads to FA overflow that initiates formation of new LDs. This mLD formation can be prevented by excess BSA in cell culture medium to sequester lipolysis-derived FA or by inhibiting FA activation by triacsin C, even in the absence of extracellular FA acceptors. Long term monitoring of LD growth during adipocyte cultivation revealed a slow transfer of neutral lipids between closely associated LDs via a "bridge" between adjacent LDs and without apparent spatial interaction over large LD surface areas.

EXPERIMENTAL PROCEDURES

Cell Culture—Cells were cultured in glass bottom dishes with a 50-mm diameter (MatTek Corp., Ashland, MA). 3T3-L1 fibroblasts were grown in Dulbecco's modified Eagle's medium (DMEM) containing 4.5 g/liter glucose and L-glutamine (Invitrogen) supplemented with 10% fetal calf serum (FCS) (Sigma-Aldrich) and antibiotics (DMEM+/+) under standard conditions (37 °C, humidified atmosphere, 5% CO_2). Two days after confluence, medium was changed to DMEM+/+ containing 10 μg/ml insulin (Sigma-Aldrich), 0.25 μM dexamethasone (Sigma-Aldrich), and 500 μM isobutylmethylxanthine (Sigma-Aldrich). After 3 and 5 days, medium was changed to DMEM+/+ containing 10 μg/ml and 0.05 μg/ml insulin, respectively. The day before the experiment, cells were incubated without insulin overnight. Experiments were performed on day 8 or 9 after initiation of differentiation. For electron microscopy, cells were cultured on collagen-coated (1% collagen) Alcar film (Gröpl, Inc., Tulln, Austria) placed in the glass bottom dishes.

Human adipose-derived stem cells (Invitrogen) were grown in complete MesenPro RS Medium (Invitrogen), and after reaching confluence, the medium was changed to Complete Adipogenic Differentiation Medium (Invitrogen). For long term experiments, cells were seeded in glass bottom dishes with a 35-mm diameter (Ibidi, Germany) with an additional culture insert (Ibidi) to enable four-dimensional CARS imaging over more than a week without the need for changing the medium.

Lipolytic Stimulation of Murine Adipocytes and Inhibition of Long Chain Fatty Acyl-CoA Synthetase—For stimulation of lipolysis, 10 μM forskolin (Sigma-Aldrich) was added to the medium. To study the effect of bovine serum albumin (BSA) on LD formation during lipolysis, 3T3-L1 cells were incubated with 10 μM forskolin (in DMEM), either containing 2% fatty acid-free BSA or no BSA. Incorporation of FAs into TAG was inhibited by the addition of 5 μM triacsin C (Sigma-Aldrich). First, cells were treated with triacsin C for 2 h in DMEM+/+, and then the medium was replaced by fresh DMEM containing 5 μM triacsin C, 10 μM forskolin, and either 2% fatty acid free BSA (control) or no BSA. A total medium volume of 2 ml was used in all experiments.

Analysis of Acyl-CoA Levels in Triacsin C-treated Differentiated 3T3-L1 Cells by Mass Spectrometry—Cells were differentiated for 8 days and subsequently pretreated for 2 h with various concentrations of triacsin C (1, 5, 10, or 20 μM) to test the efficacy of the drug to inhibit fatty acid activation. After inhibitor treatment, cells were further incubated for 1 h in fresh DMEM again containing various concentrations of triacsin C and 2% BSA. Acyl-CoAs were determined by on-line solid phase extraction liquid chromatography-mass spectrometry as described previously (20). In brief, buffer-suspended cells (250 μl of 50% 0.1 M KH_2PO_4 and 50% 2-propanol, prechilled to 4 °C) were added to internal standard mix (0.25 nmol of $^{13}C_{16}$-palmitoyl-CoA, 0.25 nmol of $^{13}C_{18}$-stearoyl-CoA, 0.1 nmol of $^{13}C_{18}$-oleoyl-CoA per sample). After the addition of 15 μl of saturated aqueous $(NH_4)_2SO_4$ solution and 0.25 ml of acetonitrile, the cell

suspension was homogenized on ice for 10–20 s using an ultrasonic homogenizer. The homogenate was vigorously mixed and centrifuged at 2500 × *g* for 10 min at 4 °C, and the supernatant was transferred to autosampler vials. Extracts were stored at −80 °C prior to analyses on an Ultimate 3000 System (Dionex, LC Packings, Sunnyvale, CA) consisting of an autosampler with cooled tray and a column oven with a switching unit coupled to an LTQ Orbitrap XL (Thermo Scientific, Waltham, MA). A Phenomenex Strata X 2.0 × 20-mm cartridge (Torrance, CA) and a Waters XBridge column (2.1 × 50 mm, 2.5 μm) (Milford, MA) were used for on-line solid phase extraction and as an analytical column, respectively. Positive electrospray ionization-mass spectrometry was performed by high resolution mass spectrometry (scan range 500–1500 *m*/*z*, resolution 60,000).

Biochemical Analysis of Fatty Acid Release—For determination of free FAs, aliquots of the corresponding media were collected, and free FA content was determined using a commercial analysis kit (WAKO Chemicals GmbH, Neuss, Germany). Cells were lysed in 0.3 M NaOH, 0.1% SDS, and protein concentration was determined using BCA reagent (Pierce).

Fluorescence Microscopy—Imaging of fluorescently labeled structures was performed on a Leica SP5 confocal microscope using a ×40, NA 1.25 oil immersion objective. LDs of 3T3-L1 cells were labeled by adding LD540 (21) to the culture medium (final concentration 1 μg/ml). The neutral lipid-specific dye LD540 was a kind gift from Christoph Thiele (Max Planck Institute of Molecular Cell Biology and Genetics). Labeling of neutral lipids was typically achieved after 10–15 min of incubation. LD540 fluorescence was excited at 561 nm, and emission was detected between 570 and 620 nm. For four-dimensional live cell imaging, cells were incubated in glass bottom dishes directly on the microscope stage using a PECON S-2 stage incubator (PECON, Inc.) at 37 °C and 5% CO_2. Three-dimensional image data were acquired in 30-min time intervals and with a voxel size of 90 × 90 × 300 nm (*x*/*y*/*z*). 100-nm TetraSpeck™ microspheres (Invitrogen) were used as subresolution particles for determination of detection capabilities of the fluorescence imaging system ($\lambda_{ex}/\lambda_{em}$, 561 nm/570–620 nm).

CARS Microscopy—CARS microscopy of 3T3-L1 cells was performed using a commercial setup consisting of a picosecond laser source and an optical parametric oscillator (OPO; *pico*-Emerald (APE (Berlin, Germany) and HighQ Laser (Rankweil, Austria)) integrated into a Leica SP5 confocal microscope (Leica Microsystems, Inc.). Detection of the CARS signal was achieved using 650/210 and 770/SP emission filters. The microscope was equipped with a non-descanned detector for acquisition of signals in forward CARS mode (22). To detect neutral lipids/LDs, the laser was tuned to 2845 cm^{-1}, thus enabling imaging of CH_2 symmetric stretching vibrations. For imaging, a Leica 1.25 NA, ×40 oil objective was used. For long term experiments of 3T3-L1 cells, *z*-stacks of images were taken at different time intervals, as indicated, with a voxel size of 90 × 90 × 300 nm (*x*/*y*/*z*).

Four-dimensional imaging of human adipose-derived stem cells was performed on a "home-built" CARS setup, based on a multiphoton microscope (Leica TCS SP5) and an Er:fiber laser source (Toptica FemtoFiber Pro) at a repetition rate of 40 MHz. The experiments were performed at 2845 cm^{-1} resonance frequency using the Stokes beam tuned to 998 nm with a power of 6.5 milliwatts and the pump laser tuned to 777 nm with a power of 62 milliwatts. A Leica 0.85 NA, ×40 air objective was used for focusing the excitation beams. Data were recorded in transmission type geometry (forward CARS) and were collected by a Leica 0.55 NA air condenser and transmitted through 641/75 and 680/SP (Semrock) emission filters. For long term experiments, cells were incubated directly on the microscope stage, using a live cell-imaging chamber (Stage Top Incubator, Tokai Hit, Japan), and *z*-stacks of images were recorded with a voxel size of 260 × 260 × 400 nm (*x*/*y*/*z*).

Transmission Electron Microscopy—Adipocytes were fixed in 0.1 M cacodylate buffer (pH 7.2) containing 2.5% glutardialdehyde and 2% paraformaldehyde for 30 min at room temperature. Cells were rinsed twice in 0.1 M cacodylate buffer for 1 h and postfixed in 2% osmium tetroxide in the same buffer for 1 h. After rinsing four times for 10 min in 0.1 M cacodylate buffer, specimens were dehydrated in a series of 50, 70, 90, and 100% cold acetone for 30 min each. Preparations were infiltrated by 2:1, 1:1, and 1:2 mixtures of 100% acetone and agar 100 epoxy resin (Gröpl, Inc.) and pure agar 100 epoxy resin for 4 h. Finally, cells were placed in agar 100 epoxy resin at room temperature for 8 h, transferred into embedding molds, and polymerized at 60 °C for 48 h. Ultrathin sections (70 nm) were cut with a Leica Ultracut UC6 and stained with lead citrate for 5 min and with uranyl acetate for 15 min. Images were taken on a Tecnai 20 transmission electron microscope (Fei, Inc.).

Imaging-based Quantification of LD Size—A *z*-stack of images of a selected cell was projected into a single two-dimensional image using maximum intensity projection. The diameter of ~50 LDs was measured using the line measure feature implemented in ImageJ (23), and surface and volume data were calculated.

Statistical Analysis of FA Release—Data are represented as mean values and S.D. from three independent experiments. Group differences were calculated using unpaired Student's *t* test (two-tailed). Levels of statistical significance were considered as follows: $p < 0.05$ (*), $p < 0.01$ (**), and $p < 0.001$ (***).

RESULTS

Lipolytic Stimulation of 3T3-L1 Adipocytes Causes Rapid Shrinkage of LDs without Detectable LD Fragmentation—To investigate the effect of lipolysis on LD size and subcellular distribution, differentiated 3T3-L1 adipocytes were labeled with LD540, stimulated with forskolin, and analyzed over time by four-dimensional live cell imaging. Already within 30 min after initiation of lipolysis, a clear shrinkage of LDs was detectable. Notably, all monitored LDs showed a progressive response to lipolytic stimulation, independent of their size or subcellular position (Fig. 1). Moreover, degradation of LD contents appeared to be correlated with the size of the organelles. Computed values for the half-life of the volume of selected LDs during lipolysis indicate that smaller LDs are faster degraded than larger LDs (Fig. 3*A*). Five hours after stimulation of lipolysis, LDs in most cells were almost completely depleted. Quite notably, no fragmentation of existing LDs was detectable under our experimental conditions, neither at the beginning of the experiment nor at later stages, when the TAG stores were almost

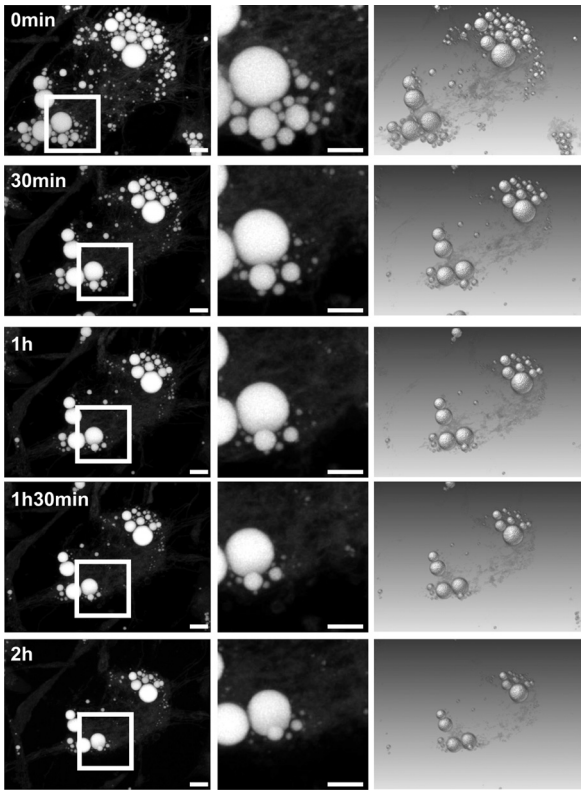

FIGURE 1. **Four-dimensional live cell imaging of LD consumption in 3T3-L1 adipocytes.** All imaged LDs decrease their size significantly within 2 h after stimulation of lipolysis by forskolin. In addition, the cell contract with progressing LD breakdown as indicated by the LD540 "background" signal and decreased cell area. No fragmentation or dispersion of LDs is observed during lipolysis. *Left*, maximum intensity projections of three-dimensional data acquired at the indicated time points; *middle*, enlarged area enclosed by the *white rectangular frame* shown in the *left panel*; *right*, direct volume-rendering representations. *Bar*, 10 μm.

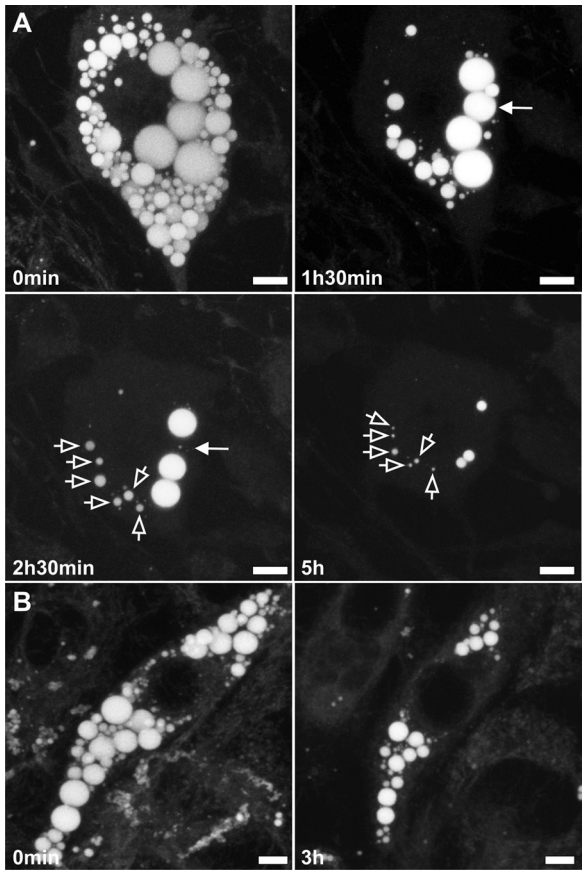

FIGURE 2. **Depletion of neutral lipid stores in 3T3-L1 adipocytes.** *A*, cell with almost totally depleted neutral lipid stores 5 h after stimulation of lipolysis using forskolin. An individual LD appears to be degraded faster than other LDs of comparable size (*solid arrows*). LDs do not significantly alter their subcellular position relative to each other during lipolysis (*open arrows*). *B*, 3T3-L1 cells stimulated with isoproterenol and isobutylmethylxanthine instead of forskolin. Similar to forskolin stimulation, LDs shrink but without detectable fragmentation or dispersion. Maximum intensity projections are shown of three-dimensional data acquired at the indicated time points. *Bar*, 10 μm.

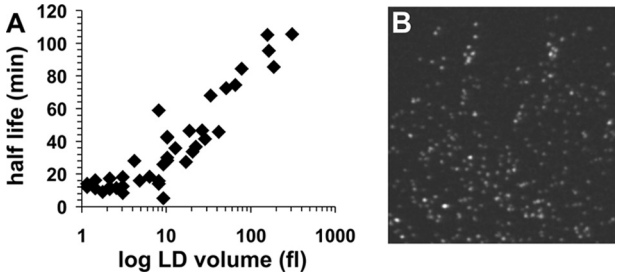

FIGURE 3. *A*, half-life of the volume of LDs upon lipolytic stimulation in 3T3-L1 adipocytes. The volume of 46 selected LDs of an individual cell was calculated based on their diameter measured in maximum intensity projections of an acquired four-dimensional data set. The half-life of the volume of LDs in stimulated cells appears to be dependent on the size of LDs. Larger LDs reach $t_{1/2}$ more slowly than smaller LDs. *B*, evaluation of the microscope setup for detection of subresolution particles. 100-nm fluorescent microspheres were imaged with the same microscope setup as used for four-dimensional imaging of 3T3-L1 cells. Groups of 100-nm beads and also individual particles are clearly detected. The image represents an enlarged area of a larger image. *Bar*, 1 μm.

entirely depleted (Figs. 1 and 2*A*). Similarly, no mLDs were observed in differentiated 3T3-L1 adipocytes that were stimulated with isoproterenol and isobutylmethylxanthine (Fig. 2*B*), demonstrating that changes in LD morphology during lipolysis were independent of the type of stimulus. As shown in a control experiment with 100-nm fluorescent subresolution beads, LDs of similar size should be clearly detectable with the microscope system used (Fig. 3*B*). This indicates that mLDs either do not occur or that their size is below the detection limit of the microscope system used. Notably, no increase in fluorescence background during lipolysis was observed, as would be expected upon the appearance of large numbers of small nano particles. Interestingly, although cell volumes significantly shrunk over time during stimulated lipolysis, most LDs appeared to remain at their relative position within the cell, suggesting that they are associated with other subcellular structures (Fig. 2*A*).

mLDs Are Synthesized de Novo—To test whether LD dynamics and morphology during lipolysis are influenced by the ability of cells to sequester excess FAs that derive from lipolysis, we omitted BSA from the culture medium, which acts as FA scavenger. In the absence of BSA, existing LDs indeed decreased in size upon forskolin-stimulated lipolysis, indicating activation of lipolysis (Fig. 4, *A* and *B*). However, FA release from adipocytes was reduced by ~90%, compared with cells cultivated in the presence of BSA (Fig. 5*A*). Notably, the absence of BSA led to the rapid formation of a large number of small LDs (<1 μm) within 30 min after initiation of lipolysis. These LDs grew significantly in size (~1–3 μm) within the following 60–90 min (Fig. 4, *A*–*C*). Thus, mLD formation is strongly influenced by

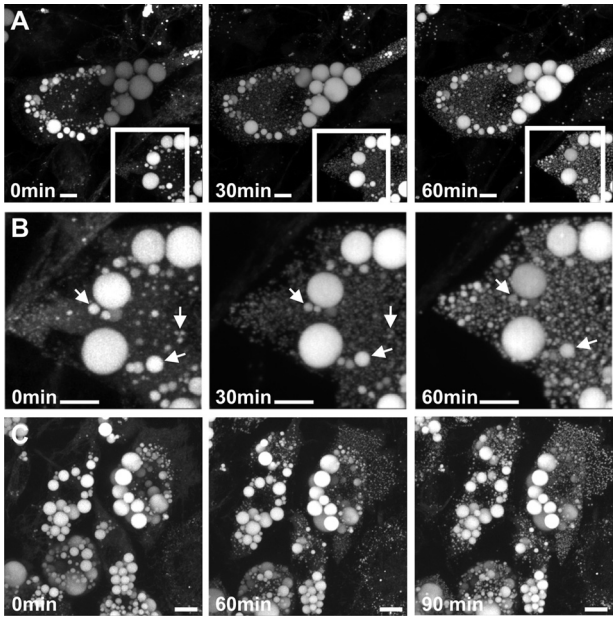

FIGURE 4. **Rapid formation of mLDs in 3T3-L1 adipocytes after stimulation of lipolysis in the absence of the extracellular fatty acid acceptor BSA.** *A*, large numbers of small LDs (<1 μm in diameter) are detected 30–60 min after hormonal stimulation. *B*, lipolysis is not inhibited in the absence of BSA (*arrows*, enlarged areas of the *white rectangular fields* shown in *A*). *Bar*, 10 μm. *C*, mLDs are formed in most cells of a cell population. Maximum intensity projections are shown of three-dimensional data acquired at the indicated time points. *Bar*, 20 μm.

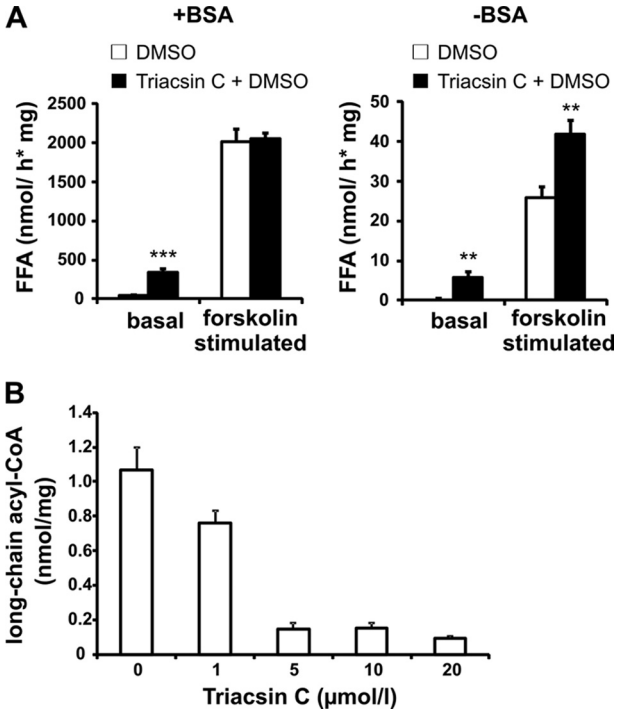

FIGURE 5. *A*, dependence of FA release on extracellular fatty acid acceptors in 3T3-L1 adipocytes. There was a >40-fold increase of FA release upon lipolytic stimulation compared with basal conditions in cells containing DMSO and BSA. There was a ~6-fold increase of FA release upon lipolytic stimulation in the presence of triacsin C and BSA (*left*). There were 80-fold (cells in DMSO) and 50-fold (cells in DMSO + triacsin C) decreases of FA release of cells cultured without fatty acid acceptors (*right*) compared with cells cultured in the presence of BSA. Results are mean ± S.D. (*error bars*) (three independent experiments). Statistical significance was determined by a two-tailed Student's *t* test (***, $p < 0.001$; **, $p < 0.01$). *B*, dose-dependent effect of triacsin C on acyl-CoA levels in differentiated (day 8) adipocytes (see "Experimental Procedures"). Maximal inhibition was achieved at 5 μM triacsin C (~−83%). Increasing concentrations of triacsin C (10 and 20 μM) did not further reduce acyl-CoA levels. Results are mean ± S.D. (two independent experiments).

the presence of the FA acceptor BSA in the culture medium during stimulated lipolysis. These newly emerging mLDs were not specifically detectable on the surface of existing LDs but were rather dispersed throughout the cell. In addition, they did not significantly change their relative subcellular position during their growth (supplemental Movie S1). Furthermore, transmission electron micrographs acquired upon lipolytic stimulation in the absence of BSA show a large number of mLDs (>1 μm) but also of nLDs (<1 μm). Again, both nLDs and mLDs are not specifically detected on the surface of larger LDs but occur dispersed in the cell (Fig. 6).

Taken together, these data suggest that formation of mLDs results from cellular FA overload in the absence of BSA in the media, which may trigger TAG (and LD) synthesis to prevent FA toxicity. Because FAs released from TAG by lipolytic degradation require activation with coenzyme A prior to (re)incorporation into lipids, we next tested whether mLD formation during stimulated lipolysis is dependent on the activity of acyl-CoA synthetases. For this purpose, we analyzed mLD formation in the presence of triacsin C, an inhibitor of acyl-CoA synthetase (24–28). To evaluate the efficacy of triacsin C in cultured adipocytes, we first determined the effect of the drug on acyl-CoA levels in 8-day differentiated 3T3-L1 cells. As shown in Fig. 5*B*, triacsin C treatment of 3T3-L1 cells led to a dose-dependent decrease in cellular acyl-CoA levels, indicative of efficient inhibition of ACS activity *in vivo*. Maximal inhibition was achieved at 5 μM triacsin C (~−83%). Thus, the increase in FA release in response to triacsin C treatment as shown in Fig. 5*A* correlates with a reduction in ACS activity.

As shown in Fig. 7, mLD formation was almost completely inhibited during stimulated lipolysis in cells treated with 5 μM

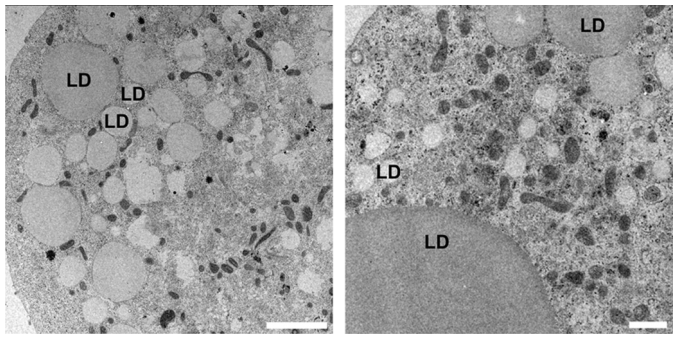

FIGURE 6. **Ultrastructural analysis of nLDs and mLDs formed upon lipolytic stimulation in 3T3-L1 adipocytes incubated in the absence of BSA.** 3T3-L1 adipocytes were treated with forskolin to stimulate lipolysis for 1 h in the absence of BSA. A single transmission electron microscopy section shows a larger number of dispersed nLDs and mLDs (*left*). Such small LDs are not detected on the surface of significantly larger LDs (>10 μm) (*right*). *Bar*, 1 μm.

triacsin C, even in the absence of the FA acceptor BSA in the medium. These data show that mLDs form *de novo* as a result of cellular FA overflow during stimulated lipolysis and that TAG degradation and new synthesis may operate in parallel to control the level of (activated) FA in the cell.

LDs Grow by Controlled Transfer of Lipids between Organelles—The molecular mechanisms that govern LD growth are currently unclear and may occur by spontaneous

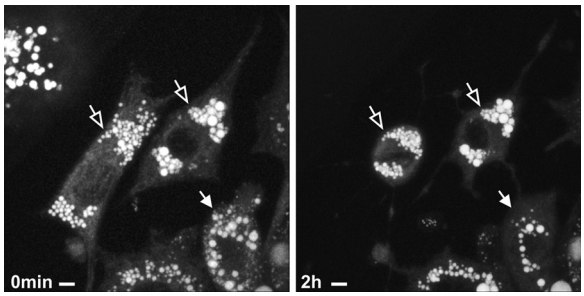

FIGURE 7. **Inhibition of mLD formation in 3T3-L1 adipocytes upon lipolytic stimulation in BSA-free medium using triacsin C.** Cells degrade their lipid droplets to some extent (*solid arrows*) or contract without significant LD consumption (*open arrows*). mLDs are not detected within 2 h of observation time. *Bar*, 10 μm. Maximum intensity projections are shown of three-dimensional data acquired at the indicated time points.

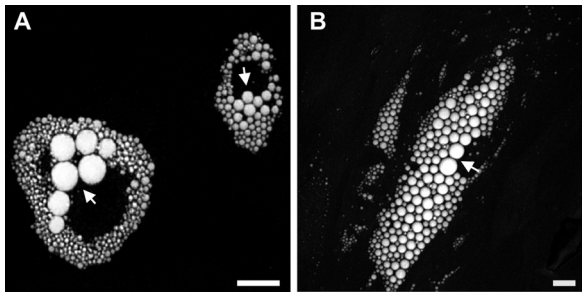

FIGURE 8. **Heterogeneity of LD size in differentiated adipocytes.** Shown are 3T3-L1 cells (*A*) and human adipose-derived stem cells differentiated into adipocytes (*B*). Large LDs (*arrows*) are frequently located near the nucleus. LDs of various sizes are scattered throughout the cytoplasm. CARS images were acquired at 2845 cm^{-1} (CH_2 symmetric stretching vibration). A maximum intensity projection is shown of acquired three-dimensional data. *Bar*, 10 μm.

homotypic fusion of individual LDs (4), by selective lipid transfer between LDs (19), or by TAG synthesis "on site" that is catalyzed by LD-resident acyltranferases (16). Subpopulations of LDs in differentiated adipocytes vary significantly in size; large LDs are frequently observed in the vicinity of the nucleus, whereas the smaller LDs form a size gradient toward the cellular periphery, both in murine 3T3-L1 cells (Fig. 8*A*) and in human adipose-derived stem cells (Fig. 8*B*). Because neutral lipid-specific fluorescent dyes tend to promote LD fusion and influence intracellular LD movement upon microscopic inspection,[5] we applied label-free CARS microscopy for long term analysis of LD growth and assembly in living cells. To accelerate LD growth, 3T3-L1 cells (day 7 after initiation of differentiation) were supplemented with oleic acid and analyzed by CARS microscopy for up to 16 h. As shown in Fig. 9 and supplemental Movie S2, several LDs grew by "absorbing" the lipid content of other, in all cases smaller, LDs. Importantly, complete lipid transfer between larger "acceptor" LDs and closely associated smaller "donor" LDs took up to several h, indicative of a finely tuned process rather than fast spontaneous fusion.

To test whether this mechanism of LD growth is induced by excess FA supply or is also occurring in untreated cells, we analyzed LD dynamics in human adipose-derived stem cells in the absence of exogenous oleic acid. Similarly to the data obtained with 3T3-L1 adipocytes in the presence of oleic acid, LDs grew by absorption of the neutral lipid content of smaller LDs also in these cells and independent of exogenous FA supply. Notably, individual LDs apparently took up the content of several other LDs, and acceptor LDs in turn served as lipid donors for others. Again, the complete absorption process of individual LDs was not a spontaneous and rapid event but rather took place over a time period of several h. (Fig. 10 and supplemental Movies S3 and S4). In summary, these observations demonstrate that lipid transfer between LDs occurs in a slow and regulated process without interaction of larger areas of the LD surfaces.

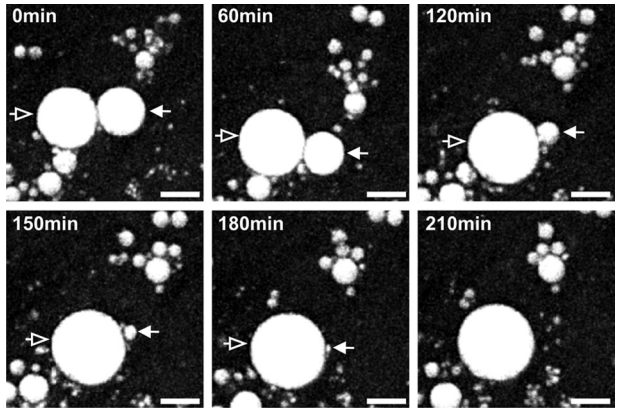

FIGURE 9. **Long term lipid transfer between LDs in 3T3-L1 adipocytes.** The large LD grows by complete "absorption" of a closely associated LD over hours. The lipid donor gets smaller over time (*solid arrows*), whereas the lipid acceptor grows over time (*open arrows*). Only small areas of the LD surfaces are closely associated during this process. The participating LDs do not significantly alter their rounded shape during lipid transfer. The process takes several h. Imaging was started 12 h after oleic acid treatment of the cells. CARS images were acquired at 2845 cm^{-1} (CH_2 symmetric stretching vibration). Maximum intensity projections are shown of three-dimensional data acquired at the indicated time points. *Bar*, 10 μm.

DISCUSSION

Understanding LD dynamics and metabolism is of great biomedical interest in view of prevalent lipid-associated disorders. Notably, LD size distribution is typically rather heterogeneous in adult adipocytes, both in cultured cell lines and in primary fat cells, such as in murine white adipose tissue (29–31). Currently, it is unclear how this heterogeneity is established and how the size distribution affects the metabolic fate of LDs. Using four-dimensional live cell imaging, we have investigated in greater detail the dynamics and morphological alterations of LDs during stimulated lipolysis as well as in metabolically active but not proliferating cells. Virtually all LDs showed a progressive loss of lipids independent of their size or subcellular position and were almost totally depleted of lipids after 5 h of persistent stimulation. We conclude that under our experimental conditions, lipolytic activity is not restricted to a subpopulation of LDs. Indeed, smaller LDs appeared to shrink faster than larger LDs, suggesting higher lipolytic activity on their surface, consistent with the increased surface/volume ratio and potentially increased density of lipase molecules on their surface. Thus, the intracellular redistribution of neutral lipids and the tendency to generate large LDs may function as an additional mechanism to regulate the rate of lipolysis. This strategy may be optimized in primary adipocytes usually containing one very large and a number of

[5] H. Wolinski and C. Jüngst, unpublished observations.

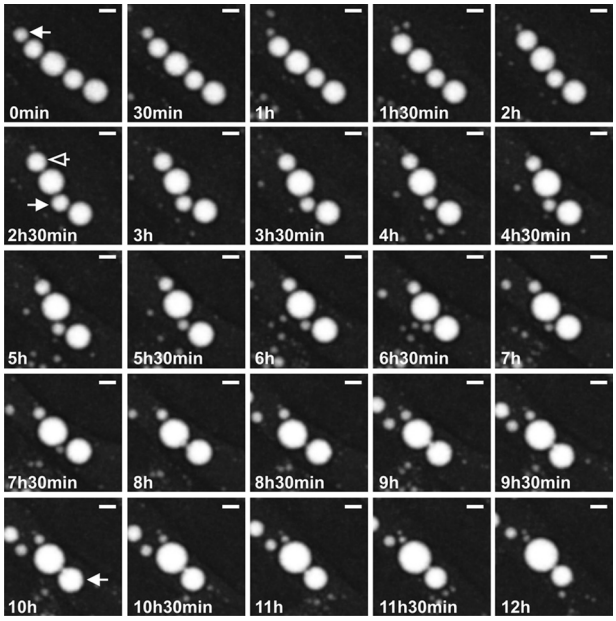

FIGURE 10. **LD growth in human adipose-derived stem cells induced to differentiate toward adipocytes is comparable with LD growth seen in 3T3-L1 cells.** Lipid acceptors can turn into lipid donors; lipid donor (*solid arrow*, *first panel*) is almost completely absorbed over time by a closely associated lipid acceptor *below*. Subsequently, this lipid acceptor in turn serves as a lipid donor (*open arrow*, *second panel*) for an LD, which simultaneously absorbs a second LD (*solid arrow*, *second panel*). Finally, this LD starts to absorb a third LD (*solid arrow*, *last panel*). Absorption of individual LDs takes more than 2 h. Again, only small fractions of the LD surfaces are closely associated during this process. CARS images were acquired at 2845 cm^{-1} (CH_2 symmetric stretching vibration). Maximum intensity projections are shown of three-dimensional data acquired at the indicated time points. *Bar*, 10 μm.

small LDs. However, the rate of degradation of LD contents is not only a function of size (surface/volume ratio) because individual LDs can occasionally be degraded significantly faster than LDs of similar size, which may be related to the differential localization of regulatory proteins. 3T3-L1 adipocytes grown in a three-dimensional matrix develop large "core" LDs and smaller peripheral LDs, which are specifically coated with perilipin (Plin1) (10). Because Plin1 is essential for the recruitment of hormone-sensitive lipase to LDs (32), it has been proposed that peripheral LDs are more sensitive to lipolytic stimulation. However, Plin1 also affects the activity of adipose triglyceride lipase (ATGL), the rate-limiting enzyme of TAG hydrolysis (33, 34). In its non-phosphorylated state, Plin1 binds the ATGL coactivator CGI-58. Upon protein kinase A (PKA) activation and phosphorylation of Plin1, CGI-58 is released and activates ATGL (35). Notably, mutations in Plin1 that fail to sequester CGI-58 have recently been shown to increase lipolysis and are associated with a novel subtype of partial lipodystrophy (36). Thus, at least under basal conditions, Plin1 can inhibit ATGL activity and the absence of this protein on core LDs may actually promote lipolysis. Moreover, the localization of Plin1 and hormone-sensitive lipase in 3T3-L1 cells is controversial because both proteins have been shown to localize to all detectable LDs under standard culture conditions (10, 37, 38).

As expected, the decrease of LD size in 3T3-L1 adipocytes in response to lipolytic stimulation resulted in a massive release of FA. Under standard lipolytic conditions (*i.e.* in the presence of the FA scavenger BSA in the culture medium), neither LD fragmentation nor the appearance of mLDs was observed, although cellular lipid stores were almost fully depleted in the course of the experiment. On the other hand, 3T3-L1 cells rapidly produced a large number of mLDs upon stimulation of lipolysis if BSA was omitted from the medium, suggesting that mLD formation is influenced by the availability of extracellular FA acceptors promoting the cellular release of FAs. Moreover, mLD formation was virtually abolished in the presence of triacsin C, an inhibitor of acyl-CoA synthetase, which is required for activation of (lipolysis-derived) FAs and their esterification into TAG. The inhibitory effect of triacsin C on FA activation is evident from the significant decrease of acyl-CoA levels and the increase of free fatty acid release under basal conditions (Fig. 5, *A* and *B*) and is also consistent with published data (39). We conclude that mLDs are newly synthesized organelles in response to cellular FA overload. Because FAs are toxic for living cells (40), re-esterification of mobilized FAs and deposition in TAG stores provides a mechanism to protect cells from FA-mediated lipotoxicity. Partial re-esterification of FAs was already shown under basal conditions (41) as well as during lipolysis in adipocytes (42). Reimport of released FAs was also suggested to cause LD dispersion under lipolytic conditions in 3T3-L1 cells (43). Similarly, LDs in hepatocytes undergo rapid lipolysis, but only a small portion of FAs is released or integrated into very low density lipoprotein. In these cells, most FAs are indeed recycled back to TAG and stored in LDs (44, 45). Furthermore, metabolic modeling studies in yeast also suggest that lipolysis and lipogenesis may indeed operate in parallel (46). Together, these observations imply that mLDs are formed *de novo* during lipolysis when FA concentrations exceed the binding capacity of extracellular BSA. Thus, the amount of BSA in the culture needs to be critically considered. In addition, the amount of intracellular FA acceptors, such as FA-binding proteins (47), might also play a role in buffering FAs and possibly influence the formation of mLDs during lipolysis.

Our study supports previous observations demonstrating that mLDs grow during lipolytic stimulation and are formed in all areas of the cell, presumably at the endoplasmic reticulum rather than at specific regions neighboring large LDs. It was hypothesized that mLDs may grow by fragmentation of existing LDs into nLDs, which may not be detectable by light microscopy, and subsequent fusion giving rise to mLDs (48). Indeed, although such small LDs cannot be resolved as single objects by light microscopy, they are still detectable based on their fluorescence staining (49) and are expected to result in a strongly increased fluorescence "background" signal. However, such an increase of the fluorescence signal was not detected in stimulated cells, neither in the presence nor in the absence of BSA. In addition, transmission electron microscopy showed a large number of mLDs and nLDs in cells stimulated for 1 h in the absence of BSA; however, these small LDs localized at a distance from the large LDs rather than close to their surfaces, which would be expected if they were derived by fragmentation. It should be noted that formation of small LDs was also observed under conditions of inhibited lipolysis, suggesting that LD fragmentation occurs independently of TAG degradation (7). This apparent discrepancy with our findings and other findings (43) remains to be resolved. Notably, mLDs did not

appear to fuse but rather grew in size by *de novo* lipid deposition. Thus, we propose that fragmentation of larger LDs into nLDs and their subsequent fusion is not required to form mLDs but rather resembles a mechanism compatible with *de novo* LD formation at specific LD/ER contact sites (16).

Spatially highly resolved light microscopy of LD dynamics in living cells is widely used due to the availability of intensely emitting, lipophilic fluorophores, such as BODIPY 493/503 or LD540 (21). We have, however, observed that fluorescent labeling may cause changes in the fusion behavior of LDs upon (extended) light exposure.[5] To prevent such light-induced alterations, we have employed CARS microscopy in this study to assess long term LD dynamics. CARS is a nonlinear optical process that allows label-free monitoring of molecular vibrations and is therefore suited for the generation of molecule-specific contrast in unlabeled samples. CARS microscopy is highly effective for detection of lipids, due to the high density of CH_2 groups in lipid molecules (22, 50, 51). Optimized excitation conditions allow CARS microscopic observations of individual unstained cells over days without detectable cell damage (52). It should be noted that LDs of sizes below ~200 nm are not visible by CARS under the chosen excitation conditions. Thus, we cannot determine whether subresolution LDs grow by a process that is different from the observed long term lipid transfer between the fat storage organelles.

Long term monitoring during adipocyte cultivation using CARS revealed a slow transfer of neutral lipids between closely associated LDs. This process was not only observed between very large LDs but also between smaller LDs (>1 μm). Strikingly, this gradual process did not require physical interaction over large LD surface areas, thus implicating that associated LDs form a channel for lipid transfer. Most notably, lipid transfer between LDs took up to several h, depending on the size of the LDs. In primary hepatocytes, a dynamic interaction between nascent and existing LDs was described that results in the transfer of neutral lipids into preformed LDs. It was hypothesized that a transient fusion and fission occurs during the contact of LDs, leading to the transfer of lipids between smaller nascent and existing larger LDs (19). The thermodynamic driving force to suck up lipids into the larger LDs is clearly defined by the tendency to minimize surface tension (*i.e.* to reduce the surface/volume ratio). However, such a transfer of lipids would require an as yet uncharacterized protein machinery that mediates LD interactions and may indeed include Rab (53) as well as SNARE (14) and motor proteins, such as dynein (12, 13). Rab18 GTPase is found both at ER membranes and on LDs in 3T3-L1 cells and other non-adipocyte cell lines (54–56), and it was suggested to represent a critical factor for establishing LD/endoplasmic reticulum associations (55). In addition, a role for Rab18 in lipogenesis and lipolysis was recently proposed. Overexpression of Rab18 in 3T3-L1 cells after insulin administration leads to an increase of TAG content and LD size, indicating that Rab18 may facilitate insulin-mediated lipid assembly into LDs. On the other hand, forskolin treatment of cells overexpressing Rab18 results in increased TAG hydrolysis in 3T3-L1 cells. Thus, Rab18 contributes in multiple ways to the regulation of lipid metabolism, perhaps as a mediator in the ER, by bringing LDs and ER structures together and thus facilitating lipid loading from the ER and/or LD fusion (57). Because LDs also harbor diacylglycerol acyltransferase activity, it could be speculated that lipid transfer between individual droplets also occurs by a deacylation/FA activation/reacylation cycle. Such a mechanism would explain the rather slow rate of lipid transfer between LDs and is compatible with the dual function of Rab18 GTPase both promoting LD fusion and lipolysis. However, because LD-associated diacylglycerol acyltransferase 2 harbors a transmembrane domain, it is controversial whether this enzyme directly resides on the LDs or LD-associated subdomains of the ER (58).

In conclusion, our findings suggest that formation of large LDs represents a regulated and slow physiological process in differentiating adipocytes, whereas mLDs form rapidly in response to cellular FA overload and are synthesized to prevent FA toxicity. We propose that LD growth requires a distinct protein machinery that mediates LD interactions, forms a channel between LDs, and thus promotes the transfer of lipids. Indeed, elegant recent evidence demonstrates that Fsp27, a member of the cell death-inducing DFF45-like effector (CIDE) family of proteins, localizes to the LD-LD interface and is involved in mediating lipid transfer between adjacent lipid droplets in 3T3-L1 cells (59, 60).

Acknowledgments—We thank Christina Eder and Viktor Adamek for technical assistance.

REFERENCES

1. Kopelman, P. G. (2000) Obesity as a medical problem. *Nature* **404,** 635–643
2. Farese, R. V., Jr., and Walther, T. C. (2009) Lipid droplets finally get a little R-E-S-P-E-C-T. *Cell* **139,** 855–860
3. Walther, T. C., and Farese, R. V., Jr. (2009) The life of lipid droplets. *Biochim. Biophys. Acta* **1791,** 459–466
4. Murphy, S., Martin, S., and Parton, R. G. (2009) Lipid droplet-organelle interactions. Sharing the fats. *Biochim. Biophys. Acta* **1791,** 441–447
5. Carman, G. M. (2012) Thematic minireview series on the lipid droplet, a dynamic organelle of biomedical and commercial importance. *J. Biol. Chem.* **287,** 2272
6. Brasaemle, D. L., and Wolins, N. E. (2012) Packaging of fat. An evolving model of lipid droplet assembly and expansion. *J. Biol. Chem.* **287,** 2273–2279
7. Marcinkiewicz, A., Gauthier, D., Garcia, A., and Brasaemle, D. L. (2006) The phosphorylation of serine 492 of perilipin A directs lipid droplet fragmentation and dispersion. *J. Biol. Chem.* **281,** 11901–11909
8. Londos, C., Brasaemle, D. L., Schultz, C. J., Segrest, J. P., and Kimmel, A. R. (1999) Perilipins, ADRP, and other proteins that associate with intracellular neutral lipid droplets in animal cells. *Semin. Cell Dev. Biol.* **10,** 51–58
9. Brasaemle, D. L., Dolios, G., Shapiro, L., and Wang, R. (2004) Proteomic analysis of proteins associated with lipid droplets of basal and lipolytically stimulated 3T3-L1 adipocytes. *J. Biol. Chem.* **279,** 46835–46842
10. Moore, H. P., Silver, R. B., Mottillo, E. P., Bernlohr, D. A., and Granneman, J. G. (2005) Perilipin targets a novel pool of lipid droplets for lipolytic attack by hormone-sensitive lipase. *J. Biol. Chem.* **280,** 43109–43120
11. Yamaguchi, T., Omatsu, N., Morimoto, E., Nakashima, H., Ueno, K., Tanaka, T., Satouchi, K., Hirose, F., and Osumi, T. (2007) CGI-58 facilitates lipolysis on lipid droplets but is not involved in the vesiculation of lipid droplets caused by hormonal stimulation. *J. Lipid Res.* **48,** 1078–1089
12. Boström, P., Rutberg, M., Ericsson, J., Holmdahl, P., Andersson, L., Frohman, M. A., Borén, J., and Olofsson, S. O. (2005) Cytosolic lipid droplets increase in size by microtubule-dependent complex formation. *Arterioscler. Thromb. Vasc. Biol.* **25,** 1945–1951
13. Andersson, L., Boström, P., Ericson, J., Rutberg, M., Magnusson, B.,

Marchesan, D., Ruiz, M., Asp, L., Huang, P., Frohman, M. A., Borén, J., and Olofsson, S. O. (2006) PLD1 and ERK2 regulate cytosolic lipid droplet formation. *J. Cell Sci.* **119,** 2246–2257
14. Boström, P., Andersson, L., Rutberg, M., Perman, J., Lidberg, U., Johansson, B. R., Fernandez-Rodriguez, J., Ericson, J., Nilsson, T., Borén, J., and Olofsson, S. O. (2007) SNARE proteins mediate fusion between cytosolic lipid droplets and are implicated in insulin sensitivity. *Nature cell biology* **9,** 1286–1293
15. Wolins, N. E., Quaynor, B. K., Skinner, J. R., Schoenfish, M. J., Tzekov, A., and Bickel, P. E. (2005) S3-12, Adipophilin, and TIP47 package lipid in adipocytes. *J. Biol. Chem.* **280,** 19146–19155
16. Kuerschner, L., Moessinger, C., and Thiele, C. (2008) Imaging of lipid biosynthesis: how a neutral lipid enters lipid droplets. *Traffic* **9,** 338–352
17. Kellner-Weibel, G., McHendry-Rinde, B., Haynes, M. P., and Adelman, S. (2001) Evidence that newly synthesized esterified cholesterol is deposited in existing cytoplasmic lipid inclusions. *J. Lipid Res.* **42,** 768–777
18. Murphy, S., Martin, S., and Parton, R. G. (2010) Quantitative analysis of lipid droplet fusion. Inefficient steady state fusion but rapid stimulation by chemical fusogens. *PLoS One* **5,** e15030
19. Wang, H., Wei, E., Quiroga, A. D., Sun, X., Touret, N., and Lehner, R. (2010) Altered lipid droplet dynamics in hepatocytes lacking triacylglycerol hydrolase expression. *Mol. Biol. Cell* **21,** 1991–2000
20. Magnes, C., Suppan, M., Pieber, T. R., Moustafa, T., Trauner, M., Haemmerle, G., and Sinner, F. M. (2008) Validated comprehensive analytical method for quantification of coenzyme A-activated compounds in biological tissues by online solid-phase extraction LC/MS/MS. *Anal. Chem.* **80,** 5736–5742
21. Spandl, J., White, D. J., Peychl, J., and Thiele, C. (2009) Live cell multicolor imaging of lipid droplets with a new dye, LD540. *Traffic* **10,** 1579–1584
22. Zumbusch, A., Holtom, G. R., and Xie, X. S. (1999) Three-dimensional vibrational imaging by coherent anti-stokes Raman scattering. *Phys. Rev. Lett.* **82,** 4142–4145
23. Girish, V., and Vijayalakshmi, A. (2004) Affordable image analysis using NIH Image/ImageJ. *Indian J. Cancer* **41,** 47
24. Omura, S., Tomoda, H., Xu, Q. M., Takahashi, Y., and Iwai, Y. (1986) Triacsins, new inhibitors of acyl-CoA synthetase produced by *Streptomyces* sp. *J. Antibiot.* **39,** 1211–1218
25. Tomoda, H., Igarashi, K., and Omura, S. (1987) Inhibition of acyl-CoA synthetase by triacsins. *Biochim. Biophys. Acta* **921,** 595–598
26. Brasaemle, D. L., Rubin, B., Harten, I. A., Gruia-Gray, J., Kimmel, A. R., and Londos, C. (2000) Perilipin A increases triacylglycerol storage by decreasing the rate of triacylglycerol hydrolysis. *J. Biol. Chem.* **275,** 38486–38493
27. Gauthier, M. S., Miyoshi, H., Souza, S. C., Cacicedo, J. M., Saha, A. K., Greenberg, A. S., and Ruderman, N. B. (2008) AMP-activated protein kinase is activated as a consequence of lipolysis in the adipocyte. Potential mechanism and physiological relevance. *J. Biol. Chem.* **283,** 16514–16524
28. Mottillo, E. P., and Granneman, J. G. (2011) Intracellular fatty acids suppress β-adrenergic induction of PKA-targeted gene expression in white adipocytes. *Am. J. Physiol. Endocrinol. Metab.* **301,** E122–E131
29. Granneman, J. G., Li, P., Lu, Y., and Tilak, J. (2004) Seeing the trees in the forest. Selective electroporation of adipocytes within adipose tissue. *Am. J. Physiol. Endocrinol. Metab.* **287,** E574–E582
30. Nagayama, M., Uchida, T., and Gohara, K. (2007) Temporal and spatial variations of lipid droplets during adipocyte division and differentiation. *J. Lipid Res.* **48,** 9–18
31. Green, H., and Kehinde, O. (1975) An established preadipose cell line and its differentiation in culture. II. Factors affecting the adipose conversion. *Cell* **5,** 19–27
32. Sztalryd, C., Xu, G., Dorward, H., Tansey, J. T., Contreras, J. A., Kimmel, A. R., and Londos, C. (2003) Perilipin A is essential for the translocation of hormone-sensitive lipase during lipolytic activation. *J. Cell Biol.* **161,** 1093–1103
33. Zimmermann, R., Strauss, J. G., Haemmerle, G., Schoiswohl, G., Birner-Gruenberger, R., Riederer, M., Lass, A., Neuberger, G., Eisenhaber, F., Hermetter, A., and Zechner, R. (2004) Fat mobilization in adipose tissue is promoted by adipose triglyceride lipase. *Science* **306,** 1383–1386
34. Wang, H., Bell, M., Sreenevasan, U., Hu, H., Liu, J., Dalen, K., Londos, C., Yamaguchi, T., Rizzo, M. A., Coleman, R., Gong, D., Brasaemle, D., and Sztalryd, C. (2011) Unique regulation of adipose triglyceride lipase (ATGL) by perilipin 5, a lipid droplet-associated protein. *J. Biol. Chem.* **286,** 15707–15715
35. Granneman, J. G., Moore, H. P., Krishnamoorthy, R., and Rathod, M. (2009) Perilipin controls lipolysis by regulating the interactions of AB-hydrolase containing 5 (Abhd5) and adipose triglyceride lipase (Atgl). *J. Biol. Chem.* **284,** 34538–34544
36. Gandotra, S., Lim, K., Girousse, A., Saudek, V., O'Rahilly, S., and Savage, D. B. (2011) Human frame shift mutations affecting the carboxyl terminus of perilipin increase lipolysis by failing to sequester the adipose triglyceride lipase (ATGL) coactivator AB-hydrolase-containing 5 (ABHD5). *J. Biol. Chem.* **286,** 34998–35006
37. Brasaemle, D. L., Levin, D. M., Adler-Wailes, D. C., and Londos, C. (2000) The lipolytic stimulation of 3T3-L1 adipocytes promotes the translocation of hormone-sensitive lipase to the surfaces of lipid storage droplets. *Biochim. Biophys. Acta* **1483,** 251–262
38. Tansey, J. T., Sztalryd, C., Hlavin, E. M., Kimmel, A. R., and Londos, C. (2004) The central role of perilipin a in lipid metabolism and adipocyte lipolysis. *IUBMB Life* **56,** 379–385
39. Lobo, S., Wiczer, B. M., and Bernlohr, D. A. (2009) Functional analysis of long-chain acyl-CoA synthetase 1 in 3T3-L1 adipocytes. *J. Biol. Chem.* **284,** 18347–18356
40. Lelliott, C., and Vidal-Puig, A. J. (2004) Lipotoxicity, an imbalance between lipogenesis *de novo* and fatty acid oxidation. *Int. J. Obes. Relat. Metab. Disord.* **28,** Suppl. 4, S22–S28
41. Bezaire, V., Mairal, A., Ribet, C., Lefort, C., Girousse, A., Jocken, J., Laurencikiene, J., Anesia, R., Rodriguez, A. M., Ryden, M., Stenson, B. M., Dani, C., Ailhaud, G., Arner, P., and Langin, D. (2009) Contribution of adipose triglyceride lipase and hormone-sensitive lipase to lipolysis in hMADS adipocytes. *J. Biol. Chem.* **284,** 18282–18291
42. Edens, N. K., Leibel, R. L., and Hirsch, J. (1990) Mechanism of free fatty acid re-esterification in human adipocytes *in vitro*. *J. Lipid Res.* **31,** 1423–1431
43. Nagayama, M., Shimizu, K., Taira, T., Uchida, T., and Gohara, K. (2010) Shrinking and development of lipid droplets in adipocytes during catecholamine-induced lipolysis. *FEBS Lett.* **584,** 86–92
44. Wiggins, D., and Gibbons, G. F. (1992) The lipolysis/esterification cycle of hepatic triacylglycerol. Its role in the secretion of very low density lipoprotein and its response to hormones and sulphonylureas. *Biochem. J.* **284,** 457–462
45. Gibbons, G. F., and Wiggins, D. (1995) *Adv. Enzyme Regul.* **35,** 179–198
46. Zanghellini, J., Natter, K., Jungreuthmayer, C., Thalhammer, A., Kurat, C. F., Gogg-Fassolter, G., Kohlwein, S. D., and von Grunberg, H. H. (2008) *FEBS J.* **275,** 5552–5563
47. Storch, J., and Thumser, A. E. (2010) *J. Biol. Chem.* **285,** 32679–32683
48. Yamaguchi, T. (2010) Crucial role of CGI-58/α/β hydrolase domain-containing protein 5 in lipid metabolism. *Biol. Pharm. Bull.* **33,** 342–345
49. Cogswell, C. J. (1995) Imaging immunogold labels with confocal microscopy. in *Handbook of Biomedical Imaging*, 2nd Ed. (Pawley, J. B., ed) pp. 507–513, Plenum Press, New York
50. Müller, M., and Zumbusch, A. (2007) Coherent anti-Stokes raman scattering microscopy. *Chemphyschem* **8,** 2156–2170
51. Evans, C. L., and Xie, X. S. (2008) Coherent anti-stokes Raman scattering microscopy. Chemical imaging for biology and medicine. *Annu. Rev. Anal. Chem.* **1,** 883–909
52. Jüngst, C., Winterhalder, M. J., and Zumbusch, A. (2011) Fast and long term lipid droplet tracking with CARS microscopy. *J. Biophotonics* **4,** 435–441
53. Bartz, R., Zehmer, J. K., Zhu, M., Chen, Y., Serrero, G., Zhao, Y., and Liu, P. (2007) Dynamic activity of lipid droplets. Protein phosphorylation and GTP-mediated protein translocation. *J. Proteome Res.* **6,** 3256–3265
54. Martin, S., Driessen, K., Nixon, S. J., Zerial, M., and Parton, R. G. (2005) Regulated localization of Rab18 to lipid droplets. Effects of lipolytic stimulation and inhibition of lipid droplet catabolism. *J. Biol. Chem.* **280,** 42325–42335
55. Ozeki, S., Cheng, J., Tauchi-Sato, K., Hatano, N., Taniguchi, H., and Fujimoto, T. (2005) Rab18 localizes to lipid droplets and induces their close apposition to the endoplasmic reticulum-derived membrane. *J. Cell Sci.*

118, 2601–2611
56. Zehmer, J. K., Huang, Y., Peng, G., Pu, J., Anderson, R. G., and Liu, P. (2009) A role for lipid droplets in intermembrane lipid traffic. *Proteomics* **9,** 914–921
57. Pulido, M. R., Diaz-Ruiz, A., Jiménez-Gómez, Y., Garcia-Navarro, S., Gracia-Navarro, F., Tinahones, F., López-Miranda, J., Frühbeck, G., Vázquez-Martínez, R., and Malagón, M. M. (2011) Rab18 dynamics in adipocytes in relation to lipogenesis, lipolysis, and obesity. *PLoS One* **6,** e22931
58. Stone, S. J., Levin, M. C., Zhou, P., Han, J., Walther, T. C., and Farese, R. V., Jr. (2009) The endoplasmic reticulum enzyme DGAT2 is found in mitochondria-associated membranes and has a mitochondrial targeting signal that promotes its association with mitochondria. *J. Biol. Chem.* **284,** 5352–5361
59. Gong, J., Sun, Z., Wu, L., Xu, W., Schieber, N., Xu, D., Shui, G., Yang, H., Parton, R. G., and Li, P. (2011) Fsp27 promotes lipid droplet growth by lipid exchange and transfer at lipid droplet contact sites. *J. Cell Biol.* **195,** 953–963
60. Jambunathan, S., Yin, J., Khan, W., Tamori, Y., and Puri, V. (2011) FSP27 promotes lipid droplet clustering and then fusion to regulate triglyceride accumulation. *PLoS One* **6,** e28614